A Spectroscopic Study of Au/$Ce_XZr_{1-X}O_2$ Catalysts

Hadma Sousa Ferreira and Maria do Carmo Rangel*
GECCAT Grupo de Estudos em Cinética e Catálise. Instituto de Química, Universidade Federal da Bahia, Campus Universitário de Ondina, Federação. 40170-280, Salvador, Bahia, Brazil

Márcio L.O. Ferreira
GECCAT Grupo de Estudos em Cinética e Catálise, Instituto de Química, Universidade Federal da Bahia, Campus Universitário de Ondina, Federação, 40170-280, Salvador, Bahia, Brazil

Iuri Pepe
Laboratório de Propriedades Óticas, Instituto de Física, Universidade Federal da Bahia, Campus Universitário de Ondina, Federação. 40 210-340, Salvador, Brazil

Antônio Ferreira da Silva
Laboratório de Propriedades Óticas. Instituto de Física. Universidade Federal da Bahia, Campus Universitário de Ondina, Federação. 40 210-340, Salvador, Brazil
(Received on 1 July, 2008)

The nature of gold species in Au/$Ce_XZr_{1-X}O_2$ catalysts was successfully investigated using the visible and near infrared photoacoustic spectroscopy and Fourier transform infrared spectroscopy of adsorbed carbon monoxide. It was found that the visible and near infrared photoacoustic spectroscopy is a powerful technique for investigating the changes of gold particle size due to addition of zirconium and the oxidation state of gold particles. It was also noted that the increase of zirconium in the solids makes gold incorporation more difficult due to the electronic shielding caused by zirconium, decreasing the probability of replacing cerium by gold. For the samples studied, the particle size ranged from 20−30 nm and the Au^+, Au^{3+} and Au^0 species were found in the catalysts.

Keywords: gold catalysts, photoacoustic spectroscopy, CO adsorbed.

INTRODUCTION

In recent years, much research effort has been devoted to the development of nanomaterials for several technological applications such as electronic devices, semiconductors, ceramic materials, electrodes for fuel cells, sensors and catalysts, among others [1-4]. Regarding catalysts, the great interest of nanostructured materials is related to their high activity as the consequence of the large surface to volume ratio of the small particles size [5-7]. Since the 1980s, when Haruta et al. [8] showed that gold particles smaller than 5 nm were catalytically active in the carbon monoxide oxidation, gold has been used to catalyze a large variety of reactions, such as carbon monoxide and hydrogen oxidation, methane oxidation, NOx reduction and water-gas shift reaction, among others [9-11].

In addition, the visible and near infrared photoacoustic spectroscopy has been successfully used for solving a wide range of problems related to surface science and catalysis [12,13]. In the present work, this technique was used for studying gold species in Au$Ce_XZr_{1-X}O_2$ catalysts. The results were consistent with those obtained by infrared spectra of chemisorbed carbon monoxide, X-ray diffraction and fluorescence energy dispersive *X*-ray.

Ceria and zirconia-supported gold catalysts have been largely investigated due to their importance for the water gas shift reaction [14]. This reaction is an important step in the low-temperature production of carbon monoxide-free hydrogen for PEM fuel cells, since carbon monoxide can irreversibly poison the electrocatalyst of the fuel cell anode [15, 16]. The numerous studies carried out on gold catalysts pointed out that the activity and especially the selectivity of gold are mainly related to particle size, oxidation state of gold and to the metal/support interactions [17, 18]. However, in spite of the large amount of works, the active form of gold for the WGS reaction remains as a subject of much discussion [19].

In this work, the nature of gold species in Au/$Ce_XZr_{1-X}O_2$ catalysts was investigated using the visible and near infrared photoacoustic spectroscopy and Fourier transform infrared spectroscopy of adsorbed carbon monoxide.

EXPERIMENTAL

Preparation of the supported gold nanoparticles

The supported gold nanoparticles were prepared by impregnating the calcined commercial supports ($Ce_{0.58}Zr_{0.42}O_2$ and $Ce_{0.70}Zr_{0.30}O_2$) with an aqueous solution (0.025 mol.L^{-1}) of hydrogen tetrachloroaurate(III)trihydrate ($HAuCl_4.3H_2O$) for 1 h. The process was carried out in a sand bath to assure the temperature uniformity of the impregnating solution. Samples were gently stirred with a glass stick. The samples were filtered and washed with ultra-pure hot water, about 50 ^{0}C, to remove chloride ions. Then, the samples were dried at 120 ^{0}C, during 12 h. After that period, the system was heated until reaching 600 ^{0}C at a heating rate of 5 ^{0}C.min^{-1} under air flow (30 mL.min^{-1}), being kept at this temperature for 2 h.

*Electronic address: mcarmov@ufba.br

Catalyst characterization

The solids prepared were characterized by fluorescence energy dispersive *X*-ray (EDX), *X*-ray diffraction (XRD), specific surface area measurements, Fourier transform infrared spectroscopy experiments using carbon monoxide as probe molecule (CO-FTIR) and near infrared photoacoustic spectroscopy (PAS).

The gold, ceria and zirconium contents in the catalysts were analyzed by fluorescence energy dispersive X-ray (EDX) technique with a Shimadzu model EDX-720. The phases in the solids were identified by X-ray diffraction experiments performed at room temperature with a Shimadzu model XD3A instrument using CuKα radiation generated at 30 kV and 20 mA, using a nickel filter.

The Brunauer-Emmett-Teller (BET) method was used to determine the specific surface area of catalysts by nitrogen adsorption/desorption at 77 K. The experiments were performed using an ASAP 2020 model equipment on samples previously heated under nitrogen (300 ^{0}C, 1 h).

The visible and near infrared photoacoustic spectroscopy (PA) experimental set-up consists of a halogen lamp used as the light source for the measurement. The polychromatic beam is diffracted by plane diffraction gratings attached to a step motor. The light beam can be numerically positioned by a personal computer interface from 350 to 1050 nm, corresponding to photons energies from about 1.2 to 3.5 eV; a set of lens and collimator produces a focused monochromatic light. This light beam is applied to the sample inside the PA closed cell, where a condenser microphone detects the light absorption intensity. An incorporated pre-amplifier enhances the microphone sensitivity. The detector output signal is applied to a lock-in amplifier that performs the synchronous signal detection, the signal amplification and noise rejection. For high reflexive sample it is possible to increase the measuring sensibility (X500) connecting a very-low noise homemade amplifier, with no compromise of the signal to noise ratio. The monochromatic output light has an intrinsic resolution, obtained by the calibration process, of 1.2 nm or 0.2%, the energy resolution is 2.8%.

Fourier transform infrared spectroscopy experiments using carbon monoxide as probe molecule (CO-FTIR) were carried out in a Perkin-Elmer model Spectrum One instrument. The sample (0.07 g) was prepared as self-supporting disc under 8 t, for 5 min. The samples were activated by heating under vacuum (10^{-6} Torr) at 200 ^{0}C, for 1 h, before the carbon monoxide admission. Then a pulse of 60 mbar of carbon monoxide for 5 min, at room temperature, was put into the self-designed infrared cell and 32 scans were accumulated with a resolution of 4 cm^{-1}.

Results and discussion

The XRD patterns of the catalysts are shown in Figure 1. The samples showed the fluorite cubic structure (Fm3m space group) [20] and the characteristic diffraction peaks shifted to higher 2θ degree with the increase of zirconium content. It reveals the decrease of lattice parameters of $Ce_XZr_{1-X}O_2$ induced by the substitution of Ce^{4+} species (0.97 Å) by Zr^{4+} small ions (0.84 Å), which indicated that the zirconium dopant is within the lattice, forming a solid solution and not as a segregate phase [15,21]. On the other hand, the XRD patterns of the catalysts showed weak diffraction lines of gold at 2 $\theta = 38.3^0$ and 44.4^0 corresponding to Au (111) and Au (200), respectively. The mean crystallite sizes of gold particles are listed in Table 1 and range from 21 nm to 30 nm. They were determined by XRD using the Scherrer equation from line broadening of Au (111).

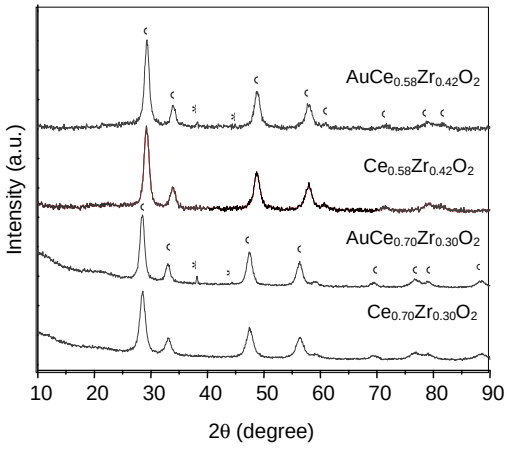

FIG. 1: XDR patterns of the supports ($Ce_XZr_{1-X}O_2$) and of the catalysts (Au/$Ce_XZr_{1-X}O_2$). (O) cubic-type structure of CeO_2 and (*) gold.

Table 1 also shows the chemical analyses results and the specific surface areas of the samples. The gold loading was lower for the $AuCe_{0.58}Zr_{0.42}O_2$ sample, indicating that some gold was not incorporated on the solid. The $Ce_{0.70}Zr_{0.30}O_2$ sample showed higher specific surface area (118 $m^2 \cdot g^{-1}$) than the $Ce_{0.58}Zr_{0.42}O_2$ support (60 $m^2.g^{-1}$). This result is on accordance with previous works [22,23] which describe that for the Ce$-$Zr binary oxides the substitution of cerium by an increasing amount of Zr^{4+} decreases the specific surface area of the mixed oxides. The deposition of gold only strongly decreased the specific surface areas of the $AuCe_{0.70}Zr_{0.30}O_2$ catalyst as compared to the support. However, the $AuCe_{0.58}Zr_{0.42}O_2$ sample showed higher specific surface area than the $AuC_{0.70}Z_{0.30}O_2$ sample, probably due to its lower gold loading, in agreement with previous work [24].

Table 1. Gold loading and specific surface areas of the samples and the mean crystallite size of gold particles.

Samples	%Au	Sg ($m^2.g^{-1}$)	Mean crystallite size (nm)
$Ce_{0.58}Zr_{0.42}O_2$	——-	60	——-
$AuCe_{0.58}Zr_{0.42}O_2$	0.51	86	21
$Ce_{0.70}Zr_{0.30}O_2$	——	118	——
$AuCe_{0.70}Zr_{0.30}O_2$	0.98	61	30

The photoacoustic (PA) characterizations started by the supports ($Ce_{0.58}Zr_{0.42}O_2$ and $Ce_{0.70}Zr_{0.30}O_2$) light absorption determination. Figure 2 shows the two supports spectra. There is no significant difference between them, unless a change on the left single band position from 320 nm, for

the $Ce_{0.70}Zr_{0.30}O_2$ sample to 370 nm for the $Ce_{0.58}Zr_{0.42}O_2$ catalyst. This band is ascribed to Ce^{3+} or Ce^{4+} species; in the last case, it is related to $O_2 \rightarrow Ce^{4+}$ charge transfer (O2p-Ce4f charge transition) [21,25,26]. The influence of Ce^{3+} species on the ceria ultraviolet and visible spectrum was investigated by several authors. The existence of a $4f^1$ electron in Ce^{3+} markedly affects the electronic spectra of the ion, producing a strong absorption in the UV range [26]. Bensalem et al. [25] showed that surface Ce^{4+} ions should be involved in localized oxygen-cerium charge transfer occurring at higher energy than that for fully coordinated cations, which leads to an increase of their polarizing power (localized effects). Ceria is a n type semiconductor with a band gap width equal to 3.1 eV, it absorbs in the UV range due to the 4f-5d transition. In pure ceria only absorption edge to the band gap is observed, that decreased in ceria-zirconia support [21,25,27]. Based on previous reports, the UV spectrum of ceria depends on the cerium content and on the particle size. When the cerium content increased a blue shift can be observed. These results may be explained by collective and localized effects [25,27].

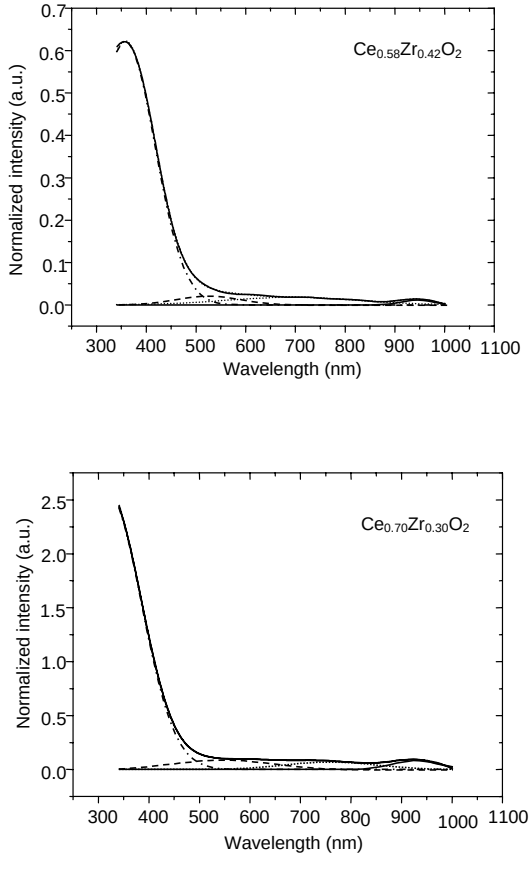

FIG. 2: Infrared photoacoustic spectroscopy (PA) spectra of the supports. (a) $Ce_{0.58}Zr_{0.42}O_2$; (b) $Ce_{0.70}Zr_{0.30}O_2$. The dashed lines represent the spectral decomposition.

Figure 3 presents the absorption spectra for the catalysts, the spectra have been normalized and their integral is the unit. For the $Ce_{0.58}Zr_{0.42}O_2$ sample, the addition of gold shows a new absorption structure centered at 520 nm, which can be related to gold species, this spectrum component is responsible for 42% of the whole sample absorption. The bump centered at 740 nm seems to be the same light absorption structure, already present in the support, but with a magnified relative contribution to the absorption spectrum. Furthermore, the 520 nm bump seems play a smaller role in the sample $AuCe_{0.58}Z_{0.42}O_2$ light absorption, these result points out the possibility of having less gold added to the support, in a proportion of about (1/3) compared to the $AuCe_{0.70}Zr_{0.30}O_2$ sample. From chemical analysis (Table 1), particularly EDX technique, was possible to determine the relative quantity of gold added to the support in both cases ($Ce_{0.58}Z_{0.42}O_2$ and $Ce_{0.70}Z_{0.30}O_2$) that number is 0.51 and 0.98%.

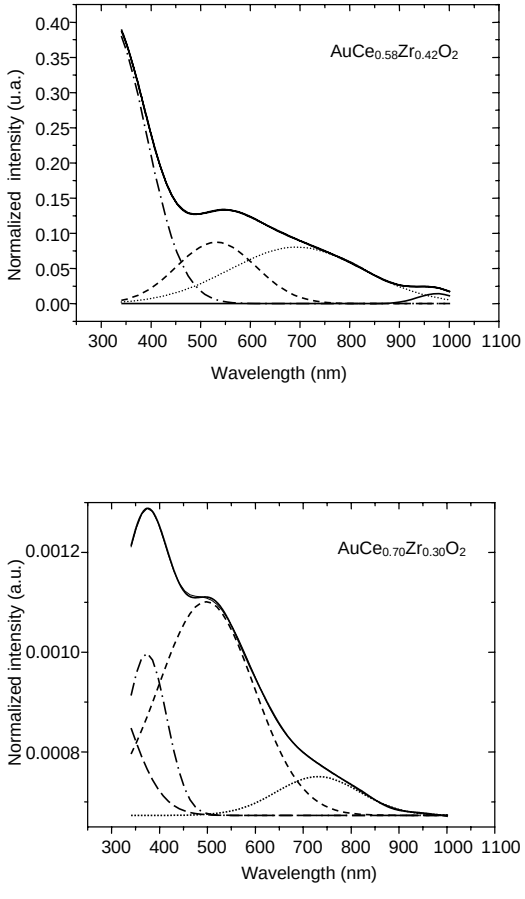

FIG. 3: Infrared photoacoustic spectroscopy (PA) spectra of the catalysts. (a) $AuCe_{0.58}Zr_{0.42}O_2$; (b) $AuCe_{0.70}Z_{0.30}O_2$. The dashed lines represent the spectral decomposition.

Those results obtained by different techniques are very consistent, which increases the reliability of the whole sample characterization process. It is important to stress that low frequency photoacoustic (from 9 to 25 Hz) has a bulk penetration and must be considered as a characterization technique and not as an analytic tool. The structure at 740 nm in $AuCe_{0.70}Zr_{0.30}O_2$ spectrum is broader in $AuCe_{0.58}Zr_{0.42}O_2$ and blue shifted, a very small band appears on the right side of this spectrum, but its poor statistics impairs any further analysis. The plasmon band centered at 500−520 nm corresponds to gold spherical nanoparticles, in good agreement with XRD results. It can be seen that the maximum peak was shifted

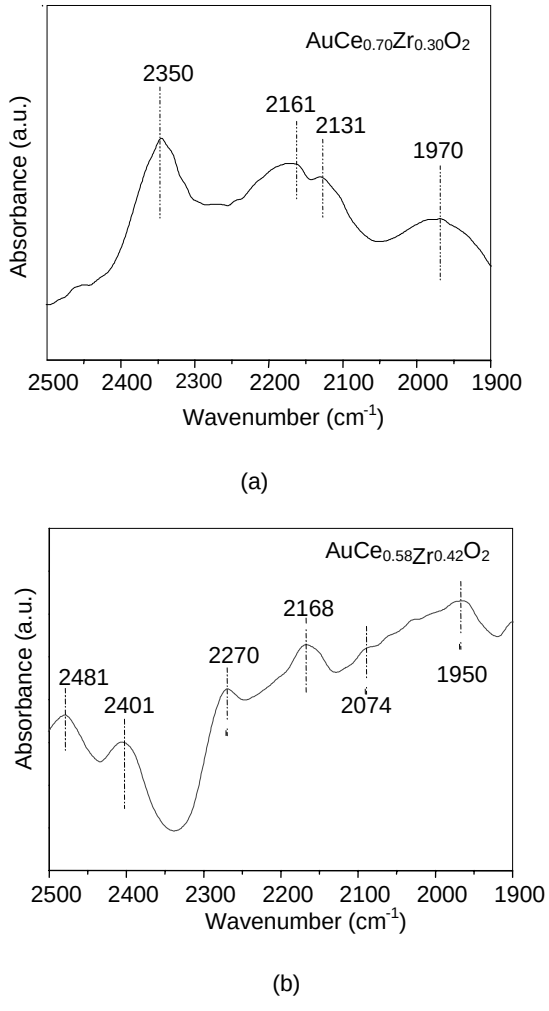

FIG. 4: FTIR spectra of chemisorbed CO on the catalysts.

to lower wavelengths with the increase of the particle size. By comparing the spectra of the catalysts, it can be noted a red shift with decreasing particle size of the 500 nm for the bigger particles to 520 nm for the smaller ones [19,24]. It is well known that the plasmon absorption spectrum of small gold particles changes depending on several physical factors such as particle size and shape and dipole-dipole interactions among particles. Also, the position and width of the gold plasmon band depend on the particle size and form [28,29].

By comparing the photoacoustic spectra of the samples one can note that the main difference between the supports and the catalysts is an absorption structure centered at 500−520 nm. For the $AuCe_{0.58}Z_{0.42}O_2$ sample, the structure is centered at 520 nm (2.34 eV) and its relative amount is 14%. On the other hand, for the $AuCe_{0.70}Zr_{0.30}O_2$ sample, it is centered at 500 nm (2.49 eV) and its relative amount is 42% of the total spectrum. From previous studies [29], the band at 560 nm has been attributed to the surface plasmon resonance of gold particles. Also, Tuzovskaya et al. [19] reported the presence of band at 250−380 nm in the spectra of as-prepared samples, which is typical of the charge transfer transitions of Au^{3+} and Au^{+} ions with the support. In our case, the support itself adsorbed in this region and the band related to gold cationic species is probably overlapped with it. Therefore, we can also conclude from the spectra that the $AuCe_{0.58}Z_{0.42}O_2$ sample has less gold that the $AuCe_{0.70}Zr_{0.30}O_2$ one which of course does not mean that the last one will be the most active catalyst. The gold proportion in the sample is 14/42, that is, only 1/3 of gold of $AuCe_{0.70}Zr_{0.30}O_2$ sample is present in the $AuCe_{0.58}Z_{0.42}O_2$ one. It means that the increase of zirconium in the support makes gold incorporation more difficult by electronic shielding caused by zirconium, decreasing the probability of replacing cerium by gold.

Figure 4 shows FTIR absorbance spectra of carbon monoxide on $AuCe_{0.58}Zr_{0.42}O_2$ and $AuCe_{0.70}Zr_{0.30}O_2$ catalysts. The adsorption of carbon monoxide after 5 min at room temperature on the as-prepared $AuCe_{0.70}Z_{0.30}O_2$ samples produces a broad band at 2350 cm^{-1}, which is characteristic of carbon dioxide interacting with the surface cations [24, 30]. This band was shifted towards higher wavenumbers in the $AuCe_{0.58}Zr_{0.42}O_2$ sample which also showed the characteristic band of carbon dioxide linearly adsorbed on Ce^{4+} sites with different coordinative unsaturation [17,27]. Moreover, in the $AuCe_{0.70}Zr_{0.30}O_2$ sample bands at 2161 cm^{-1} and 2131 cm^{-1}, assigned to carbon monoxide adsorbed on oxidized ($Au^{+}-CO$ and/or $Au^{3+}-CO$) and metallic gold (Au^{0}-CO) species respectively, were observed [24,25,28]. These bands appeared at 2168 and 2074 cm^{-1} in the $AuCe_{0.58}Zr_{0.42}O_2$ spectrum. The broad band at 1970 cm^{-1} in the $AuCe_{0.70}Zr_{0.30}O_2$ spectrum attributed to carbon monoxide adsorbed as bridge on the support cations (Ce^{4+} ions) was shifted to 1950 cm^{-1} in the other sample [29]. The band at 2270 cm^{-1} may be associated to carbonate species on ceria. These findings are in agreement with those obtained by PAS.

Conclusions

The visible and near infrared photoacoustic spectroscopy was successfully used for characterizing ceria and zirconia-supported gold catalysts. Through this technique, it was possible to infer about the change of gold particle size and shape due to addition of zirconia and also to infer about the oxidation state of gold particles. The results were in good agreements with those obtained by X-ray diffraction and Fourier transform infrared spectroscopy of carbon monoxide adsorbed on the samples. For the samples studied, the particle size ranged from 20−30 nm and the Au^{+}, Au^{3+} and Au^{0} species were found in the catalysts.

Acknowledments

HSF and MLOF acknowledge CAPES for the scholarships. The authors acknowledges the grants of FINEP, CNPq and FAPESB.

[1] M. Zäch, C. Hägglund, D. Chakarov and B. Kasemo. Curr. Opin. Solid State Mater. Sci **10**, 132 (2006).

[2] A. Helland and H. Kastenholz. J. Cleaner Production, **16**, 885 (2008).

[3] H. S. Ferreira and M.C. Rangel. *Quím. Nova.* . (in press).

[4] D.T. Thompson, Appl. Catal. A : Gen. **243**, 201 (2003).

[5] M. Harata. Catal. Today, **36**, 153 (1997).

[6] M. C. Rangel, C. L. Pieck, G. Pecchi, N. S. Fgoli and P. Reyes. Ind. Eng. Chem. Res. **40**, 5557 (2001).

[7] P. Querino, J. R. C. Bispo and M. C. Rangel. Catal. Today.**108**, 920 (2005).

[8] M. Haruta, T. Kobayashi, H. Sano and N. Yamada. Chem. Lett. **405**, (1987).

[9] G.C. Bond, C.Louis and D.Thompson. Catalysis by gold. Imperial College Press (2006).

[10] L. Ilieva, G. Pantaleo, J.W. Sobczak, I. Ivanov, A.M. Venezia and D. Andreeva. Appl. Catal. B: **76,** 107 (2007).

[11] Z.-Y. Yuan, V. Idakiev, A. Vantomme, T. Tabakova, T.-Z. Ren, and B.-L. Su. Catal. Today, **131**, 203 (2008).

[12] J. Ryczkowski. Catal. Today **124**, 11 (2007).

[13] S.-J. Kim, I.-S. Byun, H.-Y. Han, H.-L. Ju, S.H. Lee and J.-G.Choi, Appl. Catal. A:Gen. **234**, 35, (2002).

[14] W. Deng, J. de Jesus, H. Saltsburg and M. F-Stephanopoulos. Appl. Catal. A: Gen. **291**, 126 (2005).

[15] J.L. Ayastuy, M.P. G.-Marcos, A. G.-Rodrguez, J.R. G.-Velasco and M.A.G.- Ortiz. Catal. Today, **116**, 391 (2006).

[16] D.L. Trimm. Appl. Catal. A: Gen. **296**, 1 (2005).

[17] L. Delannoy, N. Weiher, N. Tsapatsaris, A. M. Beesley, L.Nchari, S.L.M. Schroeder and C. Louis.Topics in Catal. **44**, 263 (2007).

[18] T.V. Choudhary and D.W. Goodman. Appl. Catal. A: Gen. **291**, 32 (2005).

[19] I. Tuzovskava, N. Bogdanchikova, A. Simakov, V. Gurin, A. Pestryakov, M. Avalos and M. H. Faras. Chem. Phys. **338**, 23 (2007).

[20] A. Ferreira da Silva, N. Veissid, C. Y. An, I. Pepe, N. Barros de Oliveira, and A. V. Batista da Silva, Appl. Phys. Lett. **69**, 1930 (1996).

[21] A. Trovarelli, Catal. Rev. Sci. Eng. **38**, 439 (1996).

[22] M. Daturi, C. Binet, J.-C. Lavalley, A. Galtayries and R. Sporken, Chem. Phys. **1**, 5717 (1999).

[23] E. Finocchio, M. Daturi, C. Binet, J. C. Lavalley and G. Blanchard. Catal. Today. **52**, 53 (1999).

[24] I. D.- Gmez and I. Kocemba and J. M. Rynkowski. Appl. Catal. B: Environ. **83**, 240 (2008).

[25] A. Bensalem, F. Bozon-Verduraz, M. Delamar, G. Bugli. Appl.Catal. A: Gen. **121**, 81 (1995).

[26] K.J. Sreeram, R. Srinivasan, J. M. Devi, B. U. Nair and T. Ramasami. Dyes and Pigments. **75**, 687 (2007).

[27] V. Perrichon, L. Retailleu, P. Bazin, M. Daturi and J. C. Lavalley, Appl. Catal. A: Gen. **260**, 1 (2004).

[28] M. Ando, T. Kobayashi, S. Iijima and M. Haruta, Sens. Actuat. B. **96**, 589 (2003).

[29] N. Kuthirrummal, A. Dean, C. Yao and W. R. Jr. Spectrochimica Acta Part A (2007). doi:10.1016/j.saa.2007.09.011.

[30] G. Avgouropoulos, M. Manzoli, F. Boccuzzi, T. Tabakova, J. Papavasiliou, T. Ioannides and V.Idakiev. J. Catal. **0** 1, (2008). doi:10.1016/j.jcat.2008.03.014.